IEEE Access
Multidisciplinary | Rapid Review | Open Access Journal

Received November 22, 2019, accepted December 15, 2019, date of publication December 18, 2019,
date of current version January 8, 2020.

Digital Object Identifier 10.1109/ACCESS.2019.2960634

A Novel Metamaterial-Based Planar Integrated Luneburg Lens Antenna With Wide Bandwidth and High Gain

BO HU, TAO WU, YANG CAI, WEI ZHANG, AND BAO-LING ZHANG
Department of Electronic and Optical Engineering, Space Engineering University, Beijing 101416, China

Corresponding author: Yang Cai (caiyang_1991@163.com)

This work was supported by the National Natural Science Foundation of China under Grant 61901522.

ABSTRACT A novel metamaterial-based and broadband planar integrated Luneburg lens antenna is designed, fabricated, and measured. A substrate integrated waveguide (SIW) horn antenna is applied as the source to illuminate the operation of the Luneburg lens. In particular, air-via metamaterial structures are loaded in front of the SIW horn aperture to realize broadband performance. Meanwhile, the feeding structure by the SIW horn antenna and the Luneburg lens are integrated through this air-via metamaterial transition. Accordingly, the air-via unit cells are designed and arranged in an array with an equivalent gradient refractive index through diameters to achieve good wave focusing effects. Besides, a good agreement is observed between simulations and experiments. The measured results indicate that a wide bandwidth from 16 to 28 GHz is realized with the return loss below -10 dB. Moreover, high end-fire gains varying from 12.5 to 17 dBi are obtained in the band of 18-27 GHz.

INDEX TERMS Broadband, integrated, planar Luneburg lens, SIW horn antenna.

I. INTRODUCTION

Luneburg lens has the ability to transform a spherical wave on the edge of the lens into a plane wave on the opposite side. Every point on the surface of an ideal Luneburg lens is the focal point of a plane wave incident from the opposite side. This provides a Luneburg lens antenna with high gain and radial symmetry. Luneburg lens is popular for the wide-angle radiation scanning application because of its wide bandwidth, high gain and the property of forming multiple-beams. The relative permittivity of a spherical Luneburg lens is given by (1) [1]:

$$\varepsilon r(r) = n(r)^2 = 2\text{-}\left(\frac{r}{R}\right)^2 \tag{1}$$

where n is the index of refraction, r is the distance between any point in the sphere and the center of the sphere, and R is the radius of the sphere.

In fact, it is difficult to find a three-dimensional Luneburg lens in nature. Traditionally, core-shell units consisting of air and a certain dielectric were previously adopted to provide a gradually varying refractive index. However, this method suffers from complex design and processing difficulty. At present, the 3D Luneburg lens can be realized by metamaterial design and 3D printing technique [2], [3]. But high fabrication cost restricts its potential applications. To avoid the limitation of the 3D Luneburg lens, the 2D Luneburg lens with low profile, lightweight, and easy fabrication characteristics show the broad prospect. Recently the planar Luneburg lenses have been designed and fabricated to provide broadband and high-gain function by different metamaterial units [4]–[6]. But the Luneburg lens and feeding source are not integrated currently, which suffers from some problems, such as electromagnetic (EM) loss, large volume, and complex design. Hence, there is still a lack of comprehensive investigation on the integration of the Luneburg lens.

In this paper, an integrated planar Luneburg lens antenna based on metamaterial is proposed. The integration of the Luneburg lens and a feeding source is achieved by arrays of air-via structures [7], where the good transition of the incident electromagnetic wave between them is achieved. Moreover, air-via elements of variable size are distributed on the planar substrate to satisfy the gradient index function of the Luneburg lens. The proposed antenna configuration is integrated, lightweight and the experimental result agrees well with the simulation result, which shows the wide bandwidth and high gain properties.

The associate editor coordinating the review of this manuscript and approving it for publication was Haiwen Liu.

II. FEEDING STRUCTURE DESIGN

The metamaterial-based Luneburg lens antenna is designed for millimeter-wave applications. It is constructed on a single substrate with the dielectric constant of 2.5 and thickness of 4.318 mm ($\lambda_0/3$), as illustrated in Fig. 1. A waveguide-fed SIW horn antenna is placed in front of the Luneburg lens to act as a feeding structure. Considering the thickness of the substrate, the narrow impedance bandwidth, and high loss would be exhibited when using the methods of microstrip or coaxial feeding. Therefore, a symmetric wedge, which constructed with the horn antenna, is adopted to achieve a good transition between the rectangle waveguide and the SIW horn antenna [8], [9].

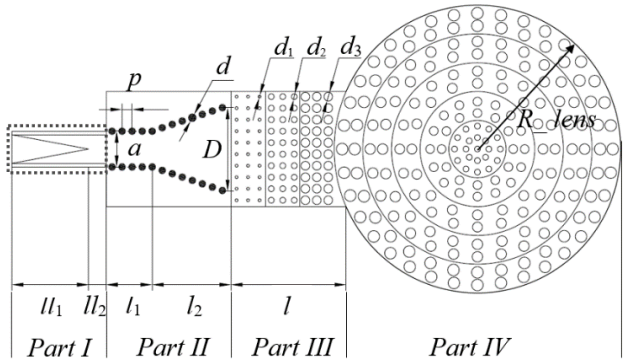

FIGURE 1. Geometry of the Luneburg lens antenna. (Physical dimensions: $ll_1 = 22$ mm, $ll_2 = 2.2$ mm, $a = 12.27$ mm, $d = 1.6$ mm, $p = 2$ mm, $d_1 = 0.87$ mm, $d_2 = 1.15$ mm, $d_3 = 1.3$ mm, $l_1 = 10.5$ mm, $l_2 = 24$ mm, $D = 32$ mm, $l = 18$ mm, R_*lens* = 31 mm).

A smooth transition between the feeding source and the Luneburg lens could be possibly obtained when a dielectric slab is placed in front of the horn aperture. The slab is divided into three blocks with the same size. And the air-vias with different diameters are perforated periodically in the dielectric slab extended from the horn aperture [10], [11]. Thus, the loading dielectric slab could be regarded as the impedance transformer between the lens and the antenna. Referring to [12], an extraction model of the equivalent refractive index for a unit cell is set, as illustrated in Fig. 2. A single air-via unit is a square dielectric with the length of m with a circular aperture with the radius of d_i drilled in the center. The equivalent refractive index calculated through the use of High Frequency Structure Simulator (HFSS) can be obtained as [13], [14]

$$\Gamma = \frac{S_{11}^2 - S_{21}^2 + 1}{2S_{11}} \pm \sqrt{\left(\frac{S_{11}^2 - S_{21}^2 + 1}{2S_{11}}\right)^2 - 1} \quad (2)$$

$$e^{-jkm} = \frac{S_{21}^2 - S_{21}^2 + 1}{2S_{21}} \pm \sqrt{\left(\frac{S_{21}^2 - S_{21}^2 + 1}{2S_{21}}\right)^2 - 1} \quad (3)$$

$$Z_{eff} = \sqrt{\frac{\mu_{eff}}{\varepsilon_{eff}}} = \frac{1+\Gamma}{1-\Gamma} \quad (4)$$

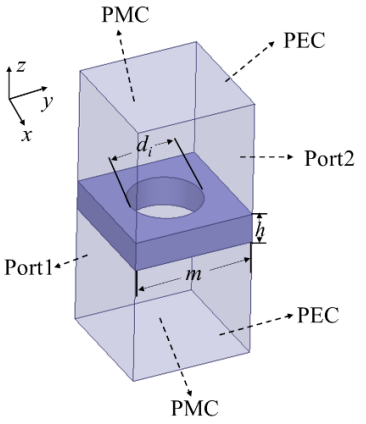

FIGURE 2. Configuration of the air-via unit of the Luneburg lens.

$$n_{eff} = -\frac{1}{jk_0 m}\left[\ln\left|e^{-jkm}\right| + j(angle(T) + 2n\pi)\right], n = 0, \pm 1, \cdots \quad (5)$$

It is demonstrated that the equivalent refractive index is the function of the diameter of the air-via in Fig. 3. As the diameter varies, the continuous equivalent refractive index could be achieved.

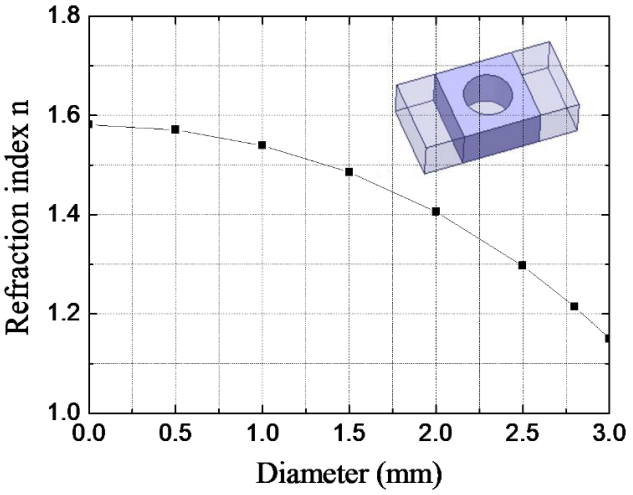

FIGURE 3. The refraction index of the substrate perforated with cylindrical air-via.

The equivalent circuit diagram of the proposed Luneburg lens antenna is depicted in Fig. 4. Z_{0L} is the characteristic impedance of the Luneburg lens, and Z_s is the impedance of the SIW horn antenna. Since Z_{0L} is much higher than Z_s, a strong impedance mismatch will be generated at the aperture if no transition is loaded. Z_{0i} represents the characteristic impedance of the transitions with different steps perforated with air-vias, which can be calculated by

$$Z_{0i} = \sqrt{\frac{\mu}{\varepsilon i}} \quad (6)$$

where εi is the effective dielectric constant of the dielectric slab with different diameter of the air-via and μ is nearly

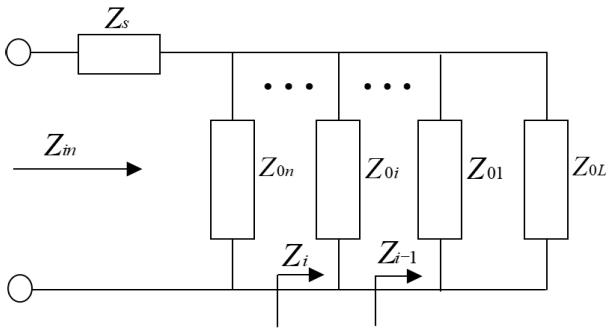

FIGURE 4. Equivalent circuit diagram of the proposed Luneburg lens antenna.

constant in the simulation. Therefore, the larger the diameter of the air-via is, the higher the impedance is obtained.

To realize a good performance of the transition, the arrangement of the air-vias should be made precisely. In our design, it has been numerically found that the phase center of the SIW horn antenna is located at a distance of 18 mm from the lens periphery. Thus, air-vias with different arrangements are perforated in a slab based on a certain length, as shown in Fig. 5. The transitions with different steps are placed between the SIW horn antenna and the metamaterial-based Luneburg lens, which is introduced in Sections III. Fig. 6 depicts the simulated $|S_{11}|$ results for different step transitions of the Luneburg lens antenna. It can be observed that the impedance matching can be improved when the transition step increases to three-step.

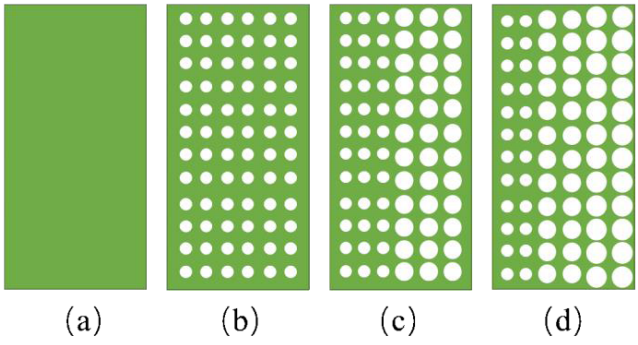

FIGURE 5. The geometry of the slab with different arrangements of the air-vias. (a) no transition. (b) one-step transition. (c) two-step transition. (d) three-step transition.

III. LUNEBURG LENS DESIGN

Based on the analysis of Section II, the structure of air-via can be used for the basic unit of the Luneburg lens to achieve the refractive index ($1 \leq n \leq \sqrt{2}$). The radius of the Luneburg lens antenna is chosen to be 31 mm, which corresponds to 2.5 λ_0 (λ_0 is the free space wavelength) at the center of the frequency band (24 GHz).

In view of the complexity of fabrication and the overall size, the Luneburg lens, based on the method of constant

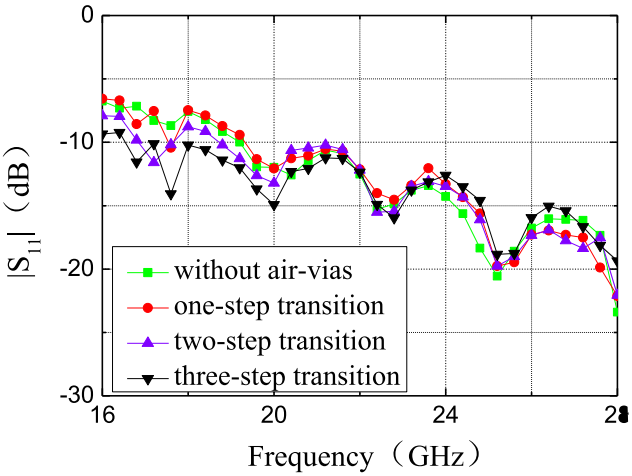

FIGURE 6. Simulated $|S_{11}|$ results for transitions with different steps of the Luneburg lens antenna.

thickness [15], is divided into five concentric regions to provide various refractive indexes respectively. As the number of regions increases, a smoother variation of the refractive indexes is realized, while the size of the Luneburg lens is increased at the same time. On the contrary, as the number of regions decreases, the variation of the refractive indexes becomes sharper, leading to the worse focusing effects of the Luneburg lens. In our design, we make a compromise of choosing five regions, the variation of the refractive index is relatively smooth and the overall size of the Luneburg lens is compact. To be consistent with the five discrete regions with different refractive indexes, different diameter values of the unit cell within five regions are determined according to considerable simulation results at the center frequency, as listed in Table 1. Hence, the final refractive index of the lens varies from 1.18 to 1.41.

TABLE 1. Diameter of air-vias and their effective index in the different zones of the luneburg lens.

Zone	d	n_{eff}
1	2.80	1.18
2	2.54	1.28
3	2.31	1.34
4	2.14	1.38
5	1.95	1.41

To verify the contribution from Luneburg lens, simulated $|S_{11}|$s of the antenna loaded with and without the lens are compared, as shown in Fig. 7. When the Luneburg lens is loaded, the bandwidth is significantly broadened by more than 15%. Fig. 8 illustrates the simulation results of the far-field radiation patterns with planar dielectric lens, Luneburg lens and without lens at 24 GHz, respectively. The simulated antenna gain of the Luneburg lens antenna is 16.3 dBi and half-power beamwidth (HPBW) is 16 degrees in the E-plane. On the other hand, the simulated gain of the antenna with the planar dielectric lens is 14.4 dBi and HPBW is 18 degrees.

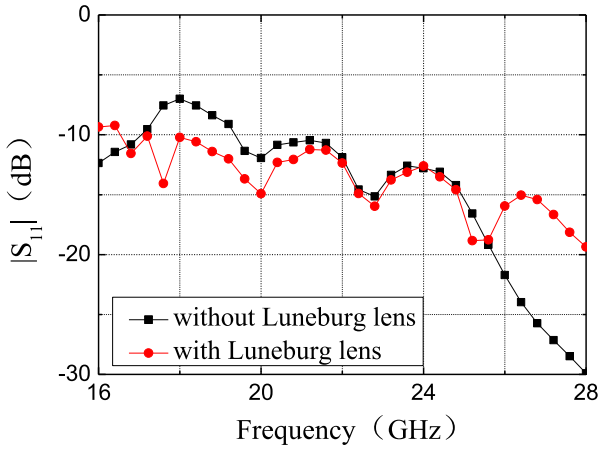

FIGURE 7. Comparison of $|S_{11}|$s of antennas with and without the Luneburg lens.

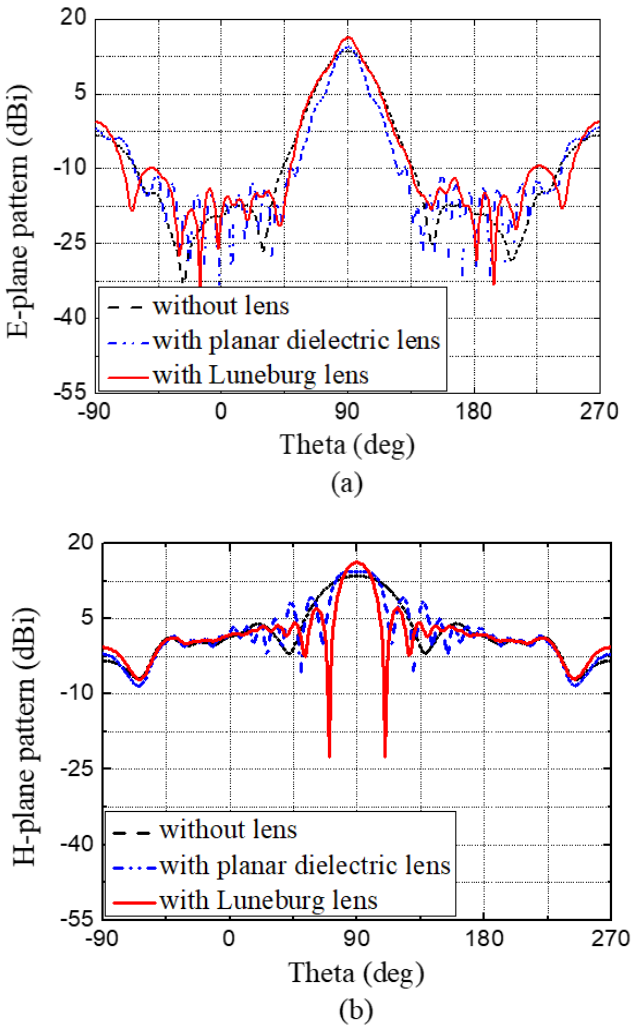

FIGURE 8. The simulated radiation patterns of the antennas with planar dielectric lens, Luneburg lens and without lens, respectively. (a) E-plane. (b) H-plane.

Meanwhile, the simulated gain of the antenna without lens is 13.5 dBi and HPBW is 28 degrees. For the Luneburg lens antenna, the simulated HPBW is 20 degrees in the H-plane,

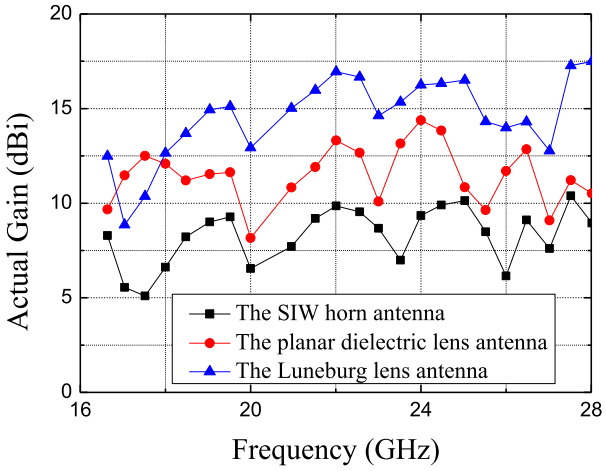

FIGURE 9. Comparison of maximum radiating gains of the antenna with and without the Luneburg lens.

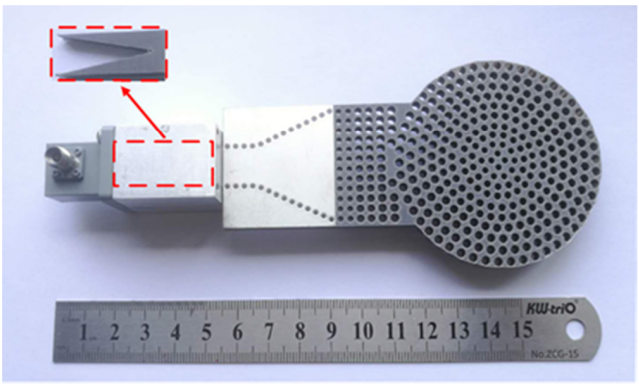

FIGURE 10. Photograph of the fabricated prototype.

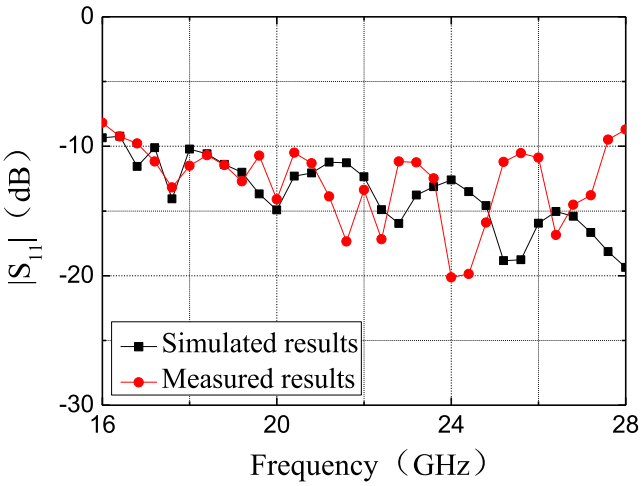

FIGURE 11. Simulated and measured $|S_{11}|$s of the Luneburg lens antenna.

while the simulated HPBW of the antenna with the planar dielectric lens is 34 degrees and the HPBW of the antenna without lens increases to 48 degrees. Therefore, the excellent radiation performance of the Luneburg lens antenna has been demonstrated.

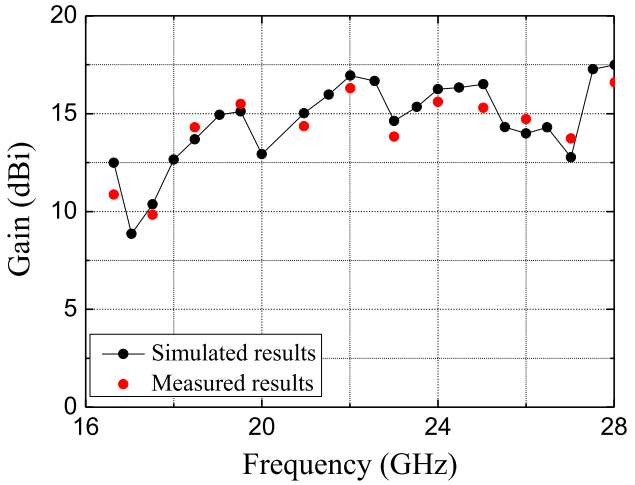

FIGURE 12. Simulated and measured gains of the proposed antenna.

Besides, as indicated by Fig. 9, the gain response with variation from 8.9 to 17 dBi is obtained in the band ranging from 16 to 28 GHz for the Luneburg lens antenna, while the traditional SIW horn antenna with the variation from 5 to 10.3 dBi is obtained. Besides, the variation from 8 to 14.4 dBi of the SIW horn antenna with a planar dielectric lens is obtained. It can be observed that a significant enhancement of actual gain is realized when an additional Luneburg lens is loaded.

IV. EXPERIMENTAL RESULTS

Based on the above analyses, a prototype of the proposed metamaterial-based integrated Luneburg lens antenna is fabricated via standard PCB technique, as shown in Fig. 10. The proposed Luneburg lens antenna connecting a waveguide-coaxial converter is assembled and measured in the near-field scanning system to verify the property. The measured and simulated $|S_{11}|$ results for the Luneburg lens antenna are presented in Fig. 11. The measured impedance bandwidth is about 46% from 16 to 28 GHz. The simulated and measured gains of the proposed antenna versus frequency are plotted in Fig. 12. It can be observed that the results agree well.

Fig. 13 illustrates the simulated and measured far-field radiation patterns in both H-plane and E-plane of four typical frequencies as 18, 20, 24, and 26 GHz. It can be seen that these measured results are in consistency with the simulation results and further prove the effectiveness of our proposed two-dimensional design, thus guaranteeing its practical application to detect the direction of incoming waves. The sidelobes are below -10 dBi for the measured results. However, small disparities with the simulated results are noticed around the sidelobes. This is attributed to field leakage in the experimental setup. It is noted that the measured E-field data shows the disagreements at 24 and 26 GHz on account of the limitation of the measurement conditions.

V. CONCLUSION

We proposed a novel planar integrated Luneburg lens antenna based on air-via metamaterial units. A simulated study has been conducted along the air-via unit cell to obtain a detailed refractive index on the individual geometry of the unit. In this way, the Luneburg lens and transformer are designed carefully by arranging various units to form the desired gradient

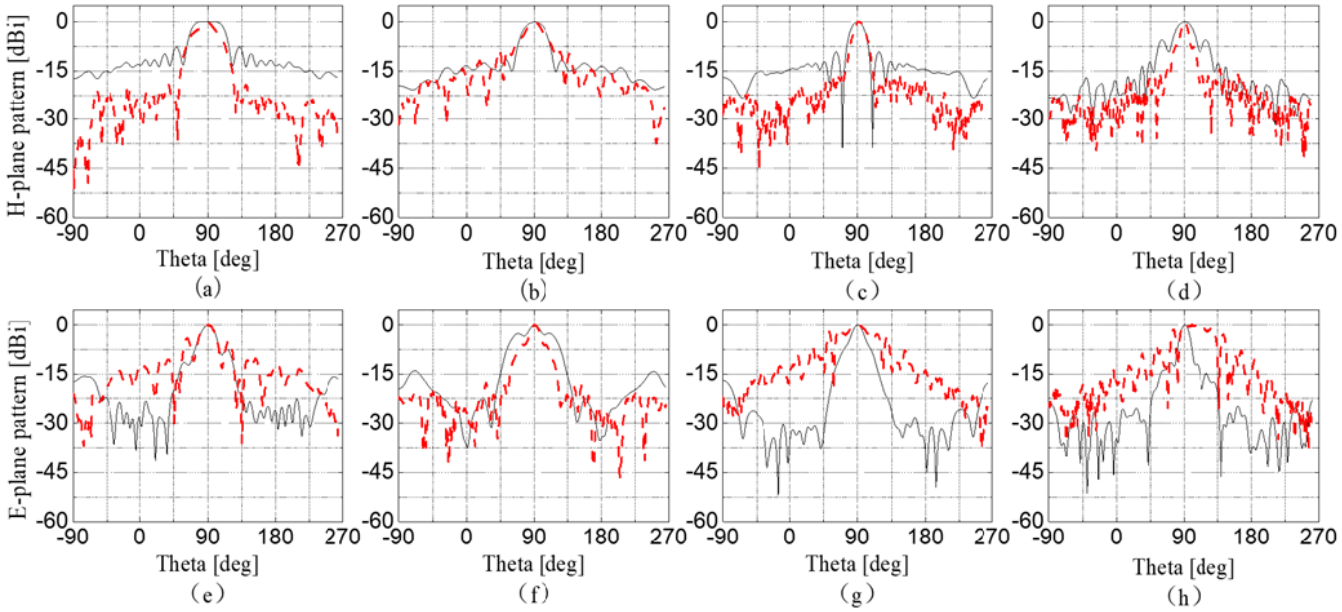

FIGURE 13. The simulated and measured radiation patterns of the proposed Luneburg lens antenna. (a) H-plane at 18 GHz. (b) H-plane at 20 GHz. (c) H-plane at 24 GHz. (d) H-plane at 26 GHz. (e) E-plane at 18 GHz. (f) E-plane at 20 GHz. (g) E-plane at 24 GHz. (h) E-plane at 26 GHz. (Straight lines denote the simulated results and dashed lines denote the measured results).

index array. In addition, a prototype has been fabricated at a low cost. Further validated by the measurement, the Luneburg lens can offer a high gain and wide bandwidth in the band ranging from 16 to 28 GHz. Moreover, the complexity of design is reduced significantly and it can be compatible with active devices due to its low profile.

REFERENCES

[1] R. K. Luneburg and A. L. King, "Mathematical theory of optics," *Amer. J. Phys.*, vol. 34, no. 1, pp. 80–81, 1966.

[2] X. Yu, M. Liang, and H. Xin, "Performance evaluation of wideband microwave direction-of-arrival estimation using Luneburg lens," *IEEE Antennas Wireless Propag. Lett.*, vol. 16, pp. 2453–2456, 2017.

[3] A. Sayanskiy, S. Glybovski, V. Akimov, D. Filonov, P. Belov, and I. Meshkovskiy, "Broadband 3-D Luneburg lenses based on metamaterials of radially diverging dielectric rods," *IEEE Antennas Wireless Propag. Lett.*, vol. 16, pp. 1520–1523, 2017.

[4] Q. Cheng, H. F. Ma, and T. J. Cui, "Broadband planar Luneburg lens based on complementary metamaterials," *Appl. Phys. Lett.*, vol. 95, no. 18, Nov. 2009, Art. no. 181901.

[5] A. Dhouibi, S. N. Burokur, A. de Lustrac, and A. Priou, "Compact metamaterial-based substrate-integrated luneburg lens antenna," *IEEE Antennas Wireless Propag. Lett.*, vol. 11, pp. 1504–1507, 2012.

[6] G. Cheng, Y.-M. Wu, J.-X. Yin, N. Zhao, T. Qiang, and X. Lv, "Planar Luneburg lens based on the high impedance surface for effective Ku-band wave focusing," *IEEE Access*, vol. 6, pp. 16942–16947, 2018.

[7] M. Li and N. Behdad, "Wideband true-time-delay microwave lenses based on metallo-dielectric and all-dielectric lowpass frequency selective surfaces," *IEEE Trans. Antennas Propag.*, vol. 61, no. 8, pp. 4109–4119, Aug. 2013.

[8] Z. J. Chen, W. Hong, and Z. Q. Kuai, "Simulation and experiment on the transition between rectangular waveguide and substrate integrated waveguide at W-band," in *Proc. Microw. Millim-Wave Symp. China*, 2007, vol. 61, no. 8, pp. 861–863.

[9] Y. Cai, Z.-P. Qian, Y.-S. Zhang, J. Jin, and W.-Q. Cao, "Bandwidth enhancement of SIW horn antenna loaded with air-via perforated dielectric slab," *IEEE Antennas Wireless Propag. Lett.*, vol. 13, pp. 571–574, 2014.

[10] G. P. Gauthier, A. Courtay, and G. M. Rebeiz, "Microstrip antennas on synthesized low dielectric-constant substrates," *IEEE Trans. Antennas Propag.*, vol. 45, no. 8, pp. 1310–1314, Aug. 1997.

[11] J. S. Colburn and Y. Rahmat-Samii, "Patch antennas on externally perforated high dielectric constant substrates," *IEEE Trans. Antennas Propag.*, vol. 47, no. 12, pp. 1785–1794, Dec. 1999.

[12] X. Chen, H. F. Ma, X. Y. Zou, W. X. Jiang, and T. J. Cui, "Three-dimensional broadband and high-directivity lens antenna made of metamaterials," *J. Appl. Phys.*, vol. 110, no. 4, Aug. 2011, Art. no. 044904.

[13] X. Chen, T. M. Grzegorczyk, B.-I. Wu, J. Pacheco, Jr., and J. A. Kong, "Robust method to retrieve the constitutive effective parameters of metamaterials," *Phys. Rev. E, Stat. Phys. Plasmas Fluids Relat. Interdiscip. Top.*, vol. 70, no. 1, 2004, Art. no. 016608.

[14] D. R. Smith, D. C. Vier, T. Koschny, and C. M. Soukoulis, "Electromagnetic parameter retrieval from inhomogeneous metamaterials," *Phys. Rev. E, Stat. Phys. Plasmas Fluids Relat. Interdiscip. Top.*, vol. 71, Mar. 2005, Art. no. 036617.

[15] J. Sanford, "A Luneberg-lens update," *IEEE Antennas Propag. Mag.*, vol. 37, no. 1, pp. 76–79, Feb. 1995.

BO HU was born in Binzhou, Shandong, China, in September 1995. He received the B.E. degree in communication engineering from Liaocheng University, in 2018. He is currently pursuing the M.S. degree with Space Engineering University.

His current research interests include Luneburg lens antenna, substrate integrated waveguide antennas, and metamaterials for microwave applications to antennas.

TAO WU was born in Honghu, Hubei, China, in December 1981. He received the B.S., M.S., and Ph.D. degrees from the Institute of Equipment Command Technology, in 2002, 2005, and 2009, respectively.

He is currently working as an Associate Professor with Space Engineering University, Beijing, China. His research interests include aerospace measurement, control technology, and signal processing.

YANG CAI was born in Suzhou, Anhui, China, in May 1991. He received the B.S. degree in communication engineering from the PLA University of Science and Technology, Nanjing, China, in 2012, and the Ph.D. degree in electronics science and technology from Army Engineering University, Nanjing, in 2017.

Since 2017, he has been working as a Lecturer with Space Engineering University, Beijing, China. His research interests include substrate-integrated waveguide antennas, horn antennas, metamaterials, and their applications to antennas.

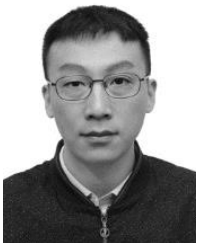

WEI ZHANG received the B.S. degree (Hons.) in communication engineering from Xidian University, Xi'an, China, in 2009, and the M.S. and Ph.D. degrees from the College of Communication Engineering, PLA University of Science and Technology, Nanjing, China, in 2012 and 2016, respectively. In 2016, he joined the Department of Electronic and Optical Engineering, Space Engineering University, Beijing, where he is currently a Lecturer. His research interests include space information networks and signal processing in TT and C systems.

BAO-LING ZHANG received the B.S. degree in radio communication from Xidian University, Xi'an, China, in 1986, and the M.S. degree in communication and electronic system from the National University of Defense Technology, China, in 1997.

She is currently an Associate Professor with Space Engineering University, Beijing, China. Her current research interests include aerospace measurement and control and information transmission.